

# A Configuration-based Compliance Modelling and Analysis Methodology for Soft Continuum Robots

Jialei Shi and Helge A. Wurdemann

**Abstract**—Soft manipulators have inherent compliant properties compared to rigid robots. This introduced compliance distributes along the body of the soft robots and varies under different configurations, which makes the compliance modelling and analysis of soft robots more complex and fundamentally different from their rigid counterparts. We propose a modelling methodology to describe the configuration-dependent compliance property of soft robots, as well as its distribution along the robots. The proposed methodology can incorporate various kinematics models and (non)linear material models then deriving the corresponding  $6 \times 6$  compliance/stiffness matrix and achieving the compliance analysis.

**Index Terms**—Soft robots, Kinematics, Compliance modelling and analysis

## I. INTRODUCTION

**T**YPICAL kinematics or dynamics models of soft robots primarily include: beam models, e.g., the Euler-Bernoulli beam model, piecewise constant curvature (PCC) model, variable curvature (VC) model, Cosserat/Kirchhoff rod model [1], [2], finite element analysis [3]. When the robots are either inextensible or have small elongation. The linear(ised) Young's modulus can be used [4]. In addition, when the robots are made of elastomers, e.g., silicone, the nonlinear hyper-elasticity shall be considered. As such, hyper-elastic models are widely utilised in soft robotics, such as the Neo-Hookean (NH) model, Mooney–Rivlin model and Yeoh model.

However, how the compliance/stiffness varies under different configuration and distributes along the robots are less investigated [5]. to qualitatively describe the configuration-dependent stiffness, experimental identification [6] has been studied. To analytically achieve the modelling, [7] proposed a method based on finite differentiation. [8] investigated how the tendons influence the overall compliance of a continuum robot. These compliance models were restricted to non-extensible robots.

In rigid-link robots, the compliance can be modelled by projecting the stiffness from the joint space to the workspace using Jacobian, but this is not applicable in soft robots since their compliance is distributed. Above all, to economically model the configuration-dependent compliance/stiffness and achieve model-based analysis of soft robots remain to be explored.

To address this gap, we propose a methodology which can describe and analyse the configuration-dependent compliance for soft continuum robots, the model structure is shown in Fig. 1(c). The methodology can incorporate various kinematics models, for instance, the PCC or Cosserat rod model. Meanwhile, the general  $6 \times 6$  compliance/stiffness matrix [9] can be derived. It is worth mentioning that the proposed methodology can accommodates both the linear material model and hyper-elastic models.

## II. METHODOLOGY

### A. Compliance/stiffness Matrices Construction

The relationship between a twist  $T$  and a wrench is  $T = CW, W = KS$ .  $C, K$  is the  $6 \times 6$  compliance and stiffness matrix, respectively, with  $C = K^{-1}$ . The continuum robot commonly is discretised into finite elements (Fig. 1(b)). The screw compliance and stiffness matrices of the  $i$ th element are denoted by  $c_i$  and  $k_i$ .  $c_i$  can be constructed by

$$c_i = \text{diag}\left[\frac{1}{GA_i}, \frac{1}{GA_i}, \frac{1}{EA_i}, \frac{1}{E(I_x)_i}, \frac{1}{E(I_y)_i}, \frac{1}{E(J_z)_i}\right], \quad (1)$$

where  $G$  is the shear modulus, and  $E$  is the Young's modulus with  $E = 2G(1 + \mu)$ ,  $\mu$  is the Poisson's ratio.  $A_i, (I_x)_i, (I_y)_i, (J_z)_i$  is the area of the cross section, moment of inertia around  $x$ -,  $y$ - and  $z$ - axes, of the  $i$ th element.

### B. Material models

1) *Linear(ised) Material model*: when the robot is inextensible, e.g., tendon-driven robot [2],  $E$  and  $G$  are constant. (1) then can be constructed based on the known dimensions.

When the robot has an elongation, a linearised  $E_l$  can be approximated via a measured strain-stress ( $\epsilon - \sigma$ ) curve, e.g., 100% Young's modulus for silicones, with  $\sigma = E_l \epsilon$ .

2) *Hyper-elasticity Model*: Hyper-elastic models are built upon the strain density function  $\Pi$  using strain invariants. The first invariant  $I_1 = \lambda_1^2 + \lambda_2^2 + \lambda_3^2$ , where the axial, circumferential and radial stretch ratio is  $\lambda_1, \lambda_2, \lambda_3$ , respectively. The second invariant  $I_2 = \lambda_1^2 \lambda_2^2 + \lambda_2^2 \lambda_3^2 + \lambda_1^2 \lambda_3^2$ . When the material is incompressible ( $\lambda_1 \lambda_2 \lambda_3 = 1$ ), the principal Cauchy stress constitutive model yields

$$\sigma_{1,t} = 2(\lambda_1^2 - \frac{1}{\lambda_1})\left(\frac{\partial \Pi}{\partial I_1} + \frac{1}{\lambda_1} \frac{\partial \Pi}{\partial I_2}\right), \quad (2)$$

where  $\sigma_{1,t}$  is the true axial stress. The difference of various hyper-elastic models is how to construct  $\Pi$ , e.g, in the NH model,  $W = \frac{\mu_0}{2}(I_1 - 3)$ . Since  $\lambda = 1 + \epsilon$ , (2) can be implicitly denoted by  $\sigma_{1,t} = f(\epsilon)$ , the exact Young's modulus can be calculated via differentiating  $f(\epsilon)$ . This yields  $E = \frac{df(\epsilon)}{d\epsilon}$ .

### C. Configuration-based Compliance Modelling

1) *Kinematics*: Here, the Cosserat rod model is adopted to exemplify the methodology. The equilibrium of the motion is [2]

$$n_s(s) = -f_e(s), \quad m_s(s) = -\hat{p}_s(s)n(s) - l_e(s). \quad (3)$$

The rotation and translation of robots can be described by

$$p_s(s) = R(s)v(s), \quad R_s(s) = R(s)\hat{u}(s), \quad (4)$$

where  $s \in [0, L]$  is the arc of manipulator's backbone (see Fig. 1(a)),  $(\cdot)_s$  denotes the derivative of  $(\cdot)$  w.r.t arc  $s$ .  $P(s)$  is the position vector.  $R(s)$  is the rotation matrix.  $n(s)$  and  $m(s)$  are the internal force and moment, respectively.  $f_e(s)$  and  $l_e(s)$  are the distributed external force and moment.  $v(s)$

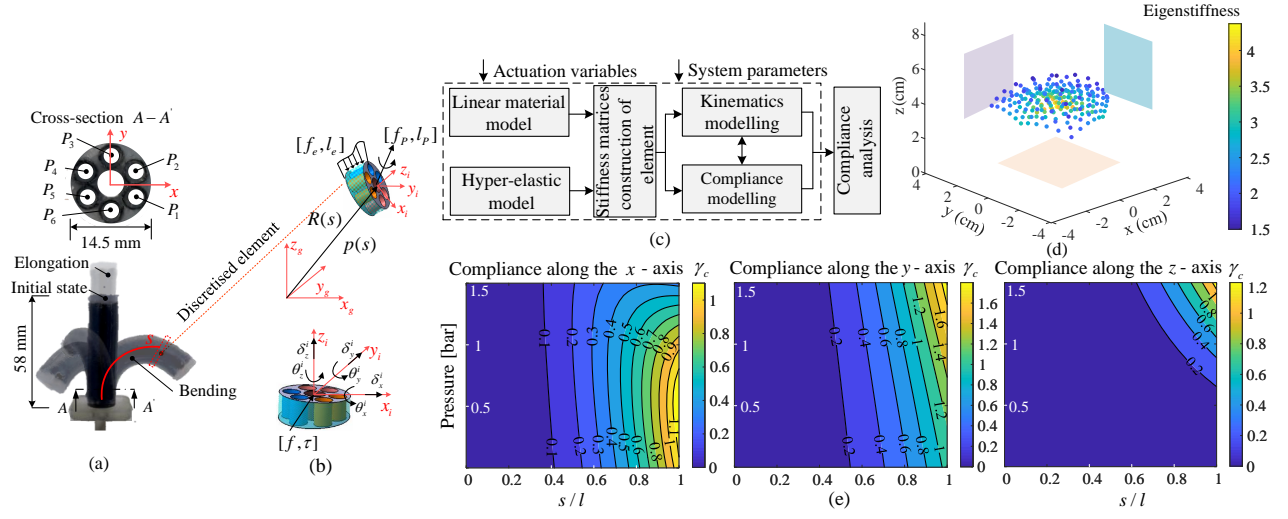


Fig. 1. (a) The soft manipulator. (b) The discretised element. (c) The structure of the proposed methodology. (d) The stiffness distribution in workspace. (e) The distribution of the dimensionless flexural compliance  $\gamma_c$  along the robot when  $P_1$  and  $P_2$  are actuated.  $\gamma_c = C_f \frac{3EI}{L^3}$  [8],  $C_f$  is the compliance value.

and  $u(s)$  are the strain and the curvature.  $\hat{(\cdot)}$  is the mapping from  $\mathbb{R}^3$  to  $\mathfrak{so}(3)$ .

The constitutive equations are

$$\begin{cases} n(s) = R(s)k_{se}(v(s) - v^*(s)) \\ m(s) = R(s)k_{bt}(u(s) - u^*(s)), \end{cases} \quad (5)$$

where  $u^*(s)$  and  $v^*(s)$  denotes the initial curvature and strain.  $k_{se} = \text{diag}[GA, GA, EA]$ ,  $k_{bt} = \text{diag}[EI_x, EI_y, GJ_z]$ .

2) *Compliance Modelling*: Integrating the element compliance along the robot gives the totally compliance of the robot at any position by [10]

$$C_i^g = \int_0^{l_i} Ad_{gi}^{-T} c_i^b Ad_{gi}^{-1} dl, \quad (6)$$

where  $C_i^g$  is the total compliance written in the global frame at the position of the  $i$ th element, and  $l_i$  is the integration length. The corresponding stiffness matrix  $K_i^g = (C_i^g)^{-1}$ . The calculation of the compliance/stiffness matrices in the body frame is

$$C_i^b = Ad_{gi}^T C_i^g Ad_{gi}, \quad K_i^b = Ad_{gi}^{-1} K_i^g Ad_{gi}^{-T}. \quad (7)$$

Combining (3) - (6), the whole set of Ordinary Differential Equations (ODEs) are

$$\begin{cases} p_s(s) = R(s)v(s), \quad v(s) = k_{se}^{-1} R^T(s)n(s) + v^*(s) \\ R_s(s) = R(s)\hat{u}(s), \quad u(s) = k_{se}^{-1} R^T(s)m(s) \\ n_s(s) = -f_e(s) \\ m_s(s) = -\hat{p}_s(s)n(s) - l_e(s) \\ (C_i)_s^g = Ad_{gi}^{-T} c_i^b Ad_{gi}^{-1}, \end{cases} \quad (8)$$

with the integration interval as  $[0, \lambda_1 L_0]$ . This formulates the whole methodology. (6) is solved by boundary condition problem using the fourth-order Runge-Kutta method.

### III. RESULTS AND DISCUSSIONS

The soft manipulator used to validate the methodology is shown in Fig. 1(a) and pneumatically driven by three chamber pairs. Fig. 1(d) shows the distribution of the stiffness in the workspace by eigenscrew decomposition. The results show, e.g., the compliance of the robot increases about 3 times from the centre to the periphery of the workspace. Fig. 1(e) shows the distribution of the flexural compliance along the

manipulator with the pressure. The compliance along the y- and z-axis increases monotonically with the pressure. Instead, the compliance variation along the x-axis is non-monotonic.

The results show the compliance varies in workspace and along the manipulator. The elongation capability increases the overall compliance. In this abstract, the Cosserat rod model is used, the implementation of the PCC model can be found in our previous work [10].

### IV. CONCLUSION

This work proposes a configuration-based compliance modelling and analysis methodology, which can model the kinematics and compliance at the same time. Moreover, this methodology can incorporate various material models and kinematics models. One direction of the future work is to exploring different material models and investigating design variations to facilitate the design and analysis of soft robots.

### REFERENCES

- [1] R. J. Webster III and B. A. Jones, "Design and kinematic modeling of constant curvature continuum robots: A review," *Int. J. Rob. Res.*, vol. 29, no. 13, pp. 1661–1683, 2010.
- [2] J. Till, V. Aloï, and C. Rucker, "Real-time dynamics of soft and continuum robots based on Cosserat rod models," *Int. J. Rob. Res.*, vol. 38, no. 6, pp. 723–746, 2019.
- [3] C. Duriez, "Control of elastic soft robots based on real-time finite element method," in *2013 IEEE International Conference on Robotics and Automation*, 2013, pp. 3982–3987.
- [4] F. Renda, F. Boyer, J. Dias, and L. Seneviratne, "Discrete Cosserat approach for multisection soft manipulator dynamics," *IEEE Trans. Robot.*, vol. 34, no. 6, pp. 1518–1533, 2018.
- [5] G. A. Naselli and B. Mazzolai, "The softness distribution index: towards the creation of guidelines for the modeling of soft-bodied robots," *Int. J. Rob. Res.*, vol. 40, no. 1, pp. 197–223, 2021.
- [6] T. G. Thuruthel, M. Manti, E. Falotico, M. Cianchetti, and C. Laschi, "Induced vibrations of soft robotic manipulators for controller design and stiffness estimation," in *Proc. IEEE RAS EMBS Int. Conf. Biomed.*, 2018, pp. 550–555.
- [7] D. C. Rucker and R. J. Webster, "Computing Jacobians and compliance matrices for externally loaded continuum robots," in *Proc. IEEE Int. Conf. Robot. Autom.*, IEEE, 2011, pp. 945–950.
- [8] K. Oliver-Butler, J. Till, and C. Rucker, "Continuum robot stiffness under external loads and prescribed tendon displacements," *IEEE Trans. Robot.*, vol. 35, no. 2, pp. 403–419, 2019.
- [9] T. Patterson and H. Lipkin, "Structure of robot compliance," *J. Mech. Des.*, vol. 115, no. 3, pp. 576–580, 1993.
- [10] J. Shi, J. C. Frantz, A. Shariati, A. Shiva, J. S. Dai, D. Martins, and H. A. Wurdemann, "Screw theory-based stiffness analysis for a fluidic-driven soft robotic manipulator," in *Proc. IEEE Int. Conf. Robot. Autom.*, IEEE, 2021, pp. 11 938–11 944.